

# Thermal Hall Effect of Spin Waves in Frustrated Kagomé Antiferromagnets

S. A. Owerre<sup>1,2</sup>

<sup>1</sup>Perimeter Institute for Theoretical Physics, 31 Caroline St. N., Waterloo, Ontario N2L 2Y5, Canada.

<sup>2</sup>African Institute for Mathematical Sciences, 6 Melrose Road, Muizenberg, Cape Town 7945, South Africa.

(Dated: July 28, 2022)

In frustrated magnets the Dzyaloshinsky-Moriya interaction arising from spin-orbit coupling can induce a magnetic long-range order. Here we report a theoretically prediction of thermal Hall effect in frustrated kagomé magnets such as  $KCr_3(OH)_6(SO_4)_2$  and  $KFe_3(OH)_6(SO_4)_2$ . The thermal Hall effects in these materials are induced by scalar spin chirality as opposed to DMI. The scalar spin chirality originates from magnetic field-induced non-coplanar spin textures, but in general it can be spontaneously developed as a macroscopic order parameter in chiral quantum spin liquids. Therefore, there is a possibility of thermal Hall effect in frustrated kagomé magnets such as herbertsmithite  $ZnCu_3(OH)_6Cl_2$  and the chromium compound  $Ca_{10}Cr_7O_{28}$ , although they also show evidence of magnetic order in the presence of a magnetic field or pressure.

*Introduction*—. Topological phases of matter are active research field in condensed matter physics, mostly dominated by electronic systems. Quite recently the concepts of topological matter have been extended to nonelectronic bosonic systems such as quantized spin waves (magnons) [1–17] and quantized lattice vibrations (phonons) [18–23]. In the former, spin-orbit coupling (SOC) manifests in the form of Dzyaloshinsky-Moriya interaction (DMI) [24, 25] and it leads to topological spin excitations and chiral edge modes in collinear ferromagnets [5, 6]. The quantized spin waves or magnons are charge-neutral quasiparticles and they do not experience a Lorentz force as in charge particles. However, a temperature gradient can induce a heat current and the DMI-induced Berry curvature acts as an effective magnetic field in momentum space. This leads to a thermal Hall effect characterized by a temperature dependent thermal Hall conductivity [1, 3]. Thermal Hall effect is now an emerging active research area for probing the topological nature of magnetic spin excitations in quantum magnets. The thermal Hall effect of spin waves has been realized experimentally in a number of pyrochlore ferromagnets [2, 4]. Recently, DMI-induced topological magnon bands and thermal Hall effect have been observed in collinear kagomé ferromagnet  $Cu(1-3, bdc)$  [8, 9]. These materials are believed to be useful for designing systems with low-dissipation applicable to spin-based computing or magnon spintronics [26].

In frustrated kagomé magnets, however, there is no magnetic long-range order (LRO) down to the lowest accessible temperatures. The classical ground states have an extensive degeneracy and they are considered as candidates for quantum spin liquids (QSL) [27, 28]. The ground state of spin-1/2 Heisenberg model on the kagomé lattice is believed to be a  $U(1)$ -Dirac spin liquid [29]. In physical realistic materials, however, there are other interactions and perturbations that tend to alleviate QSL ground states and lead to LRO. Recent experimental syntheses of kagomé antiferromagnetic materials have shown that the effects of SOC or DMI are not negligible in frustrated magnets. The DMI is an intrinsic perturbation to the Heisenberg interaction which arises from SOC

and it affects the low-temperature physics of frustrated magnets. One of the striking features of the DM perturbation is that it can induce a long-range magnetic order (LRO) with a  $\mathbf{q} = 0$  propagation vector in frustrated kagomé magnets [30]. Hence, the DMI suppresses the QSL phase of frustrated kagomé antiferromagnets up to a critical value [31]. The syntheses of materials have shown that various experimentally accessible frustrated kagomé antiferromagnets show evidence of coplanar/noncollinear  $\mathbf{q} = 0$  LRO at specific temperatures [30–35]. The famous frustrated kagomé magnets with this LRO are jarosites, such as  $KCr_3(OH)_6(SO_4)_2$  [34, 35] and  $KFe_3(OH)_6(SO_4)_2$  [30, 32]. Even highly frustrated magnets with QSL ground states such as herbertsmithite  $ZnCu_3(OH)_6Cl_2$  [36] and  $Ca_{10}Cr_7O_{28}$  [37] are fragile in the presence of magnetic field or pressure and they show evidence of magnetic order [38, 39]. However, the role of DMI and magnetic field in frustrated kagomé magnets has not been investigated in the context of thermal Hall effect and topological spin excitations.

Usually, the thermal Hall effect of spin excitations arises in insulating ferromagnets because the spontaneous magnetization combined with DMI break the time-reversal symmetry (TRS) macroscopically even in the absence of applied magnetic field. In this report, we show that the DMI is not the primary source of thermal Hall effect in frustrated kagomé magnets with/without LRO. Rather, field-induced scalar spin chirality provides both thermal Hall effect and topological spin excitations. In general, the presence of scalar spin chirality does not necessarily require a LRO or a magnetic field as in chiral QSL states [41–44]. Therefore our findings can be extended to a wide range of disordered phases on the kagomé lattice with spontaneous scalar spin chirality. The experimental probe for thermal Hall effect in these frustrated magnets will provide an understanding of both topological magnetic excitations and scalar spin chirality. In this respect, our results sharply contrast with collinear magnetic systems [2, 8, 9] and dimerized quantum magnets [40] in a magnetic field with finite DMI and zero scalar spin chirality.

*Model*—. We consider the Hamiltonian for frustrated kagomé antiferromagnets given by

$$\mathcal{H} = \mathcal{J} \sum_{\langle i,j \rangle} \mathbf{S}_i \cdot \mathbf{S}_j + \mathcal{J}_2 \sum_{\langle\langle i,j \rangle\rangle} \mathbf{S}_i \cdot \mathbf{S}_j + \sum_{\langle i,j \rangle} \mathbf{D}_{ij} \cdot \mathbf{S}_i \times \mathbf{S}_j. \quad (1)$$

The first summation runs over nearest-neighbours (NN) and the second runs over next-nearest-neighbours (NNN), where  $\mathcal{J}, \mathcal{J}_2 > 0$  are the isotropic antiferromagnetic couplings respectively and  $\mathbf{S}_i$  is the spin moment at site  $i$ . According to Moriya rules [25], the midpoint between two magnetic ions on the kagomé lattice is not an inversion center. Therefore the DM vector  $\mathbf{D}_{ij}$  can be allowed on the kagomé lattice as shown in Fig. 1. In ferromagnets the DMI breaks TRS and leads to topological spin waves [1–17], whereas in the present frustrated antiferromagnetic model the DMI is known to stabilize the  $120^\circ$  coplanar  $\mathbf{q} = 0$  magnetic structure [30]. Besides, the NNN coupling  $\mathcal{J}_2 > 0$  can equally stabilize the coplanar magnetic structure [46]. The out-of-plane DMI  $\mathbf{D}_{ij} = (0, 0, \mp\mathcal{D}_z)$  is intrinsic to the kagomé lattice, where  $-/+$  alternates between up/down triangles of the kagomé lattice as shown in Fig. 1. The sign of out-of-plane DMI determines the vector chirality of the coplanar  $120^\circ$  order and only one ground state is selected for each sign of the DMI [30]. The positive vector chirality in Fig. 1 with  $\mathcal{D}_z > 0$  is the ground state of most jarosites and we will consider this case. The DMI breaks the global  $SO(3)$  rotation symmetry of the Hamiltonian down to  $SO(2)$  global spin rotation symmetry in the  $x$ - $y$  plane. Depending on the frustrated kagomé magnet the in-plane DM component may vanish or negligible [31, 34–36]. When it is present, it breaks mirror reflection symmetry on the lattice and global spin rotation symmetry. It can lead to spin canting with weak out-of-plane ferromagnetic moment. However, most materials have very small or negligible in-plane DM components due to dominant out-of-plane components [31, 34–36]. Therefore its presence will not change the basic results of this report.

*Dirac magnon*—. As we mentioned above, the presence of sizeable DMI in this model has been proven to induce LRO. Nevertheless, the present model still differs significantly from collinear magnets because the DMI does not play the same role in both systems as we will show. Figure 2 shows the spin wave excitations of the  $120^\circ$  coplanar spins (see Ref. [45]) along the high symmetry points of the Brillouin zone [47] with  $\Gamma = (0, 0)$ ,  $\mathbf{M} = (\pi/2, \pi/2\sqrt{3})$  and  $\mathbf{K} = (2\pi/3, 0)$ . For  $\mathcal{J}_2 \neq 0, \mathcal{D}_z \neq 0$  there is  $SO(2)$  rotation symmetry in the  $x$ - $y$  plane. There are two dispersive bands and one nearly flat mode corresponding to a lifted zero mode. For  $\mathcal{J}_2 \neq 0, \mathcal{D}_z = 0$  the global  $SO(3)$  rotation symmetry is restored and the three dispersive bands have Goldstone modes at  $\Gamma$ . The interesting feature of this system is the linear band crossing of two magnon branches at  $\mathbf{K}$ , which realizes a two-dimensional (2D) Dirac Hamiltonian

$$\mathcal{H}(\pm\mathbf{K} + \mathbf{q}) = c_0 \mathbb{I}_{2 \times 2} + c_1 (\pm q_x \sigma_x + q_y \sigma_y), \quad (2)$$

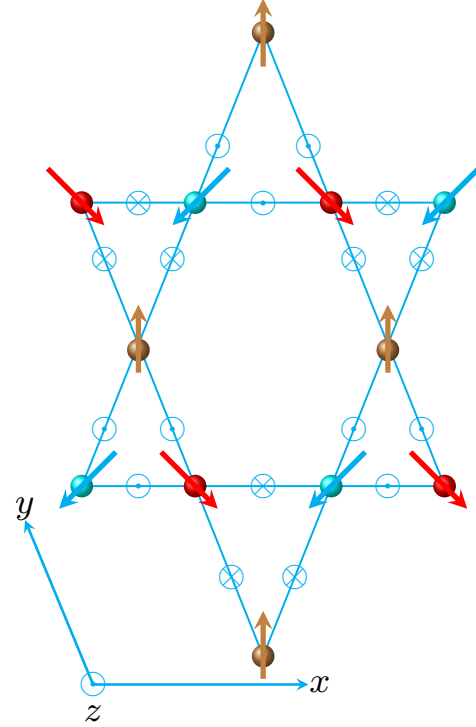


FIG. 1: **Kagomé lattice**. Coplanar  $\mathbf{q} = 0$  spin configuration on the kagomé lattice with positive vector chirality. The alternating DMI lie at the midpoint between two magnetic ions.

where  $\mathbf{q}$  is the momentum vector,  $c_0$  and  $c_1$  are functions of the Hamiltonian parameters,  $\sigma$  is a Pauli matrix and  $\mathbb{I}_{2 \times 2}$  is an identity matrix. The linearized Hamiltonian (2) has winding number  $\pm 1$  for states at  $\pm\mathbf{K}$  and it is different from the Goldstone modes of continuous rotational symmetry breaking. The presence of Dirac points in the presence of SOC (in this case DMI) is the basis of Weyl magnon [15, 16] and Dirac semimetal in electronic systems [48]. Thus, the present model can be regarded as a magnon analog of quasi-2D Dirac semimetal. From symmetry point of view, the mirror reflection symmetry with respect to the kagomé planes is a good symmetry of the kagomé lattice, but reverses the  $120^\circ$  coplanar spins and TRS brings the spins back to the original states. Hence, the combination of mirror reflection and time-reversal symmetries leaves the  $120^\circ$  coplanar spins invariant. Therefore, the Dirac points are protected by a combination of mirror reflection and time-reversal symmetries. A thorough study of Dirac magnon points with DMI is beyond the purview of this report and will be presented in detail elsewhere. For Fe-jarosites a small in-plane DMI induces a gap at  $\Gamma$  point and very small gap at  $\mathbf{K}$  point but does not remove the linear band crossing at  $\Gamma - \mathbf{K}$  line [33]. The point here is that the DMI does not lead to topological magnon bands unlike in collinear ferromagnets.

*Topological magnon*—. We expect the Dirac magnon points to be at the boundary between topological and

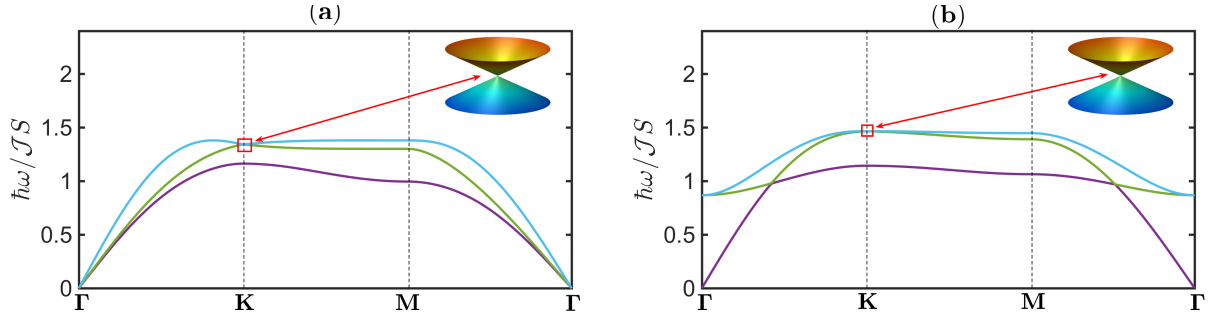


FIG. 2: **Spin wave excitations at zero magnetic field.** (a)  $\mathcal{D}/\mathcal{J} = 0$ ,  $\mathcal{J}_2/\mathcal{J} = 0.3$ . (b)  $\mathcal{D}/\mathcal{J} = 0.2$ ,  $\mathcal{J}_2/\mathcal{J} = 0.1$ . The inset shows gapless Dirac cone at  $\mathbf{K}$ .

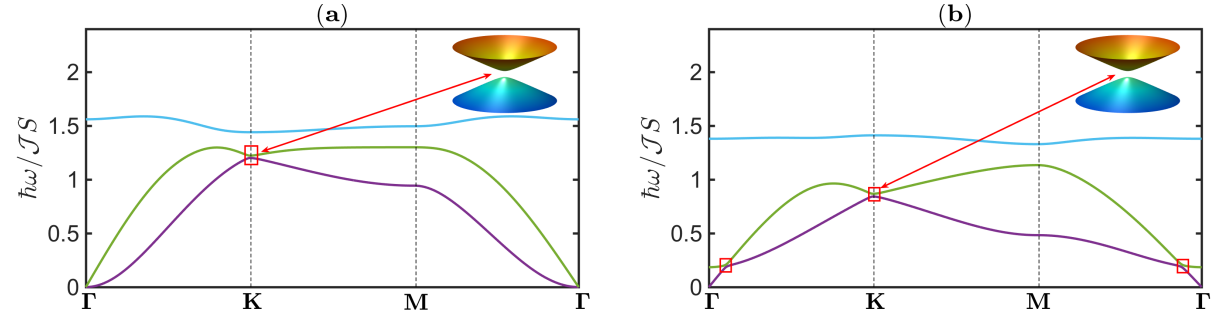


FIG. 3: **Topological spin wave excitations at nonzero magnetic field**  $h = 0.4h_s$ . (a)  $\mathcal{D}_z/\mathcal{J} = 0$ ,  $\mathcal{J}_2/\mathcal{J} = 0.3$ . (b)  $\mathcal{D}_z/\mathcal{J} = 0.06$ ,  $\mathcal{J}_2/\mathcal{J} = 0.03$  with  $\mathcal{J} = 3.34$  meV. The inset corresponds to gap magnon bands indicated by red squares.

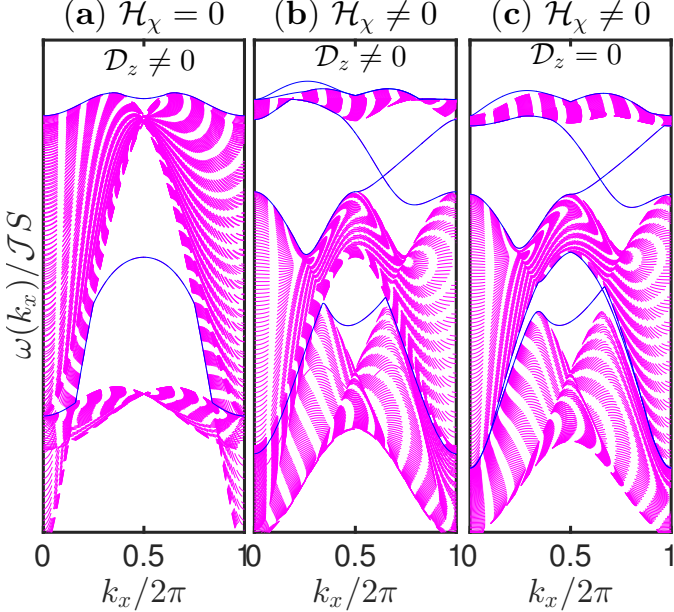


FIG. 4: **Chiral spin wave edge modes.** (a).  $h/h_s = 0$  ( $\mathcal{H}_\chi = 0$ ) with  $\mathcal{D}_z \neq 0$ . (b) with DMI.  $h/h_s = 0.4$  ( $\mathcal{H}_\chi \neq 0$ ) with DMI. (c).  $h/h_s = 0.4$  ( $\mathcal{H}_\chi \neq 0$ ) without DMI. The parameters are the same as Fig. 3. The pink lines are the bulk bands and the blue lines are the edge modes.

trivial insulators just like in electronic systems. Therefore, the system can be driven to a topological phase by breaking the symmetries that protect the Dirac magnon points. As we previously mentioned, an in-plane DMI breaks mirror reflection symmetry but preserves TRS. If the in-plane DM component is dominant it is capable of inducing topological magnon bands. However, due to a dominant out-of-plane DM component in most kagomé antiferromagnetic crystals, the value of the in-plane DM component is usually suppressed [31, 34–36]. Hence, the effects of in-plane DMI can be negligible and the Dirac magnon points will persist. The system can be driven to a topological phase by applying a magnetic field perpendicular to the kagomé plane given by  $\mathcal{H}_Z = -\mathbf{B} \cdot \sum_i \mathbf{S}_i$ , where  $\mathbf{B} = g\mu_B \mathcal{B}_z \hat{\mathbf{z}}$ ,  $g$  is the  $g$ -factor and  $\mu_B$  is the Bohr magneton. The Zeeman magnetic field induces a non-coplanar magnetic spin texture with an induced scalar spin chirality given by (see Ref. [45])

$$\mathcal{H}_\chi \sim \cos \chi \sum \mathbf{S}_i \cdot (\mathbf{S}_j \times \mathbf{S}_k), \quad (3)$$

where  $\cos \chi = h/h_s$  with  $h_s = [6(\mathcal{J} + \mathcal{J}_2) + 2\sqrt{3}\mathcal{D}_z]$  and  $h = g\mu_B \mathcal{B}_z$ . Under  $180^\circ$  rotation of the spins, the scalar chirality changes sign that is  $\mathcal{H}_\chi \rightarrow -\mathcal{H}_\chi$  as  $\chi \rightarrow \pi + \chi$ .

The most important feature of this model is that the scalar spin chirality does not require the presence of DMI. This suggests that the DMI is not the primary source of topological spin excitations in frustrated magnets, which sharply differs from collinear magnets [1–17] and triplon

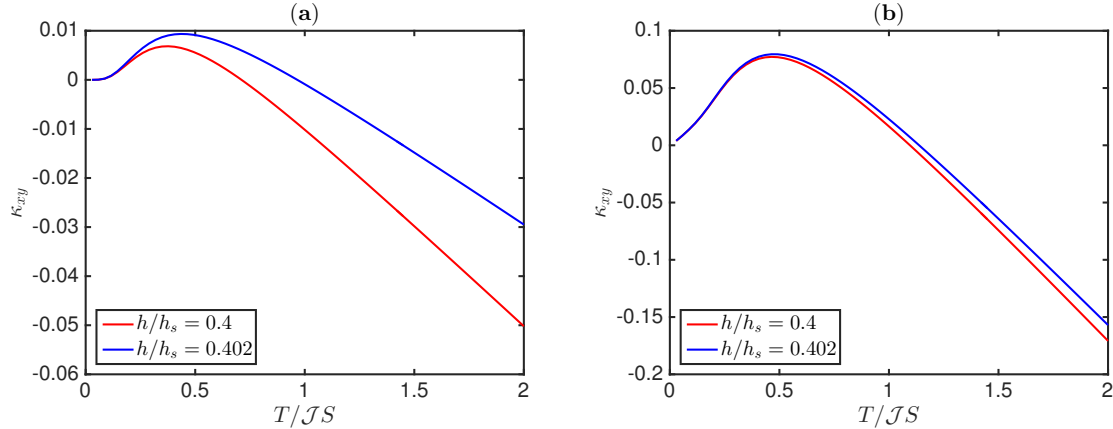


FIG. 5: **Thermal Hall effect.** Low-temperature dependence of thermal Hall conductivity  $\kappa_{xy}$ . (a)  $\mathcal{D}_z/\mathcal{J} = 0.06$ ,  $\mathcal{J}_2/\mathcal{J} = 0.03$ . (b)  $\mathcal{D}_z/\mathcal{J} = 0$ ,  $\mathcal{J}_2/\mathcal{J} = 0.3$ .

excitations [40] in a magnetic field with zero scalar spin chirality. The importance of this quantity (scalar chirality) is that it plays a crucial role in different areas of physical interest. It is the hallmark of chiral QSLs in which both time-reversal and parity symmetries are broken without any LRO  $\langle \mathbf{S}_j \rangle = 0$  [41–44]. The scalar chirality is also present in the cuboc1 phase of frustrated kagomé lattice [50]. Its main origin is due to geometrical spin frustration. The propagation of magnon around a set of three non-coplanar magnetic moments gives rise to a fictitious magnetic flux  $\Phi$  and the Berry curvature is related to the solid angle subtended by the three spins on each triangular plaquette. This defines the scalar spin chirality in momentum space (see Ref. [45]).

The magnon energy branches of the noncoplanar spin textures are shown in Fig. 3 with the parameter values of  $\text{KFe}_3(\text{OH})_6(\text{SO}_4)_2$  [33] with/without DMI. The dispersions show a finite gap at all points in the Brillouin zone. The linearized Hamiltonian for two avoided band crossings at  $\pm\mathbf{K}$  can be written as

$$\mathcal{H}(\pm\mathbf{K} + \mathbf{q}) = c_0 \mathbb{I}_{2 \times 2} + c_1 (\pm q_x \sigma_x + q_y \sigma_y) + m(\Phi) \sigma_z, \quad (4)$$

where  $m(\Phi) \propto \Phi$  and  $\sin \Phi$  is related to the scalar spin chirality. In principle, a gap Dirac point is not enough to prove that a system is topological. To further substantiate the topological nature of the system we have solved for the chiral edge modes using a strip geometry with open boundary conditions along the  $y$  direction and infinite along  $x$  direction as depicted in Fig. 4. At zero magnetic field  $\mathcal{H}_x = 0$ , there are no gapless edge modes, but a single edge mode connects the Dirac points of the dispersive bands. As the magnetic field is turned on  $\mathcal{H}_x \neq 0$ , we clearly see gapless edge modes between the upper and middle bands, which signify a strong topological magnon insulator [5]. Because of the bosonic nature of magnons there is no Fermi energy or completely filled bands in this system. Nevertheless, a Chern number can still be defined for this system as shown in (see Ref. [45]). The

Chern numbers in the topological regime are calculated as  $[0, -\text{sgn}(\sin \Phi), \text{sgn}(\sin \Phi)]$  for the lower, middle, and upper bands respectively. This confirms that the system is in the topological regime.

*Thermal Hall effect*—. Having established the topological nature of the system, now we will investigate an experimentally accessible aspect of insulating frustrated kagomé quantum magnets. The measurement of thermal Hall response using inelastic neutron scattering is the new method to probe the topological nature of spin excitations in insulating quantum magnets [2, 8, 9]. In some respects, it is analogous to quantum anomalous Hall effect in electronic systems, but requires a temperature gradient and a heat current. From linear response theory, the general formula for thermal Hall conductivity of spin excitations  $\kappa_{xy}$  can be derived, see Ref. [7]. The low-temperature dependence of  $\kappa_{xy}$  for the present model is plotted in Fig. 5(a) with the parameter values of  $\text{KFe}_3(\text{OH})_6(\text{SO}_4)_2$  [32]. At zero magnetic field there is no thermal Hall effect in accordance with the analysis of topological spin waves and edge modes discussed above. The crucial features of this model is that for zero DMI  $\mathcal{D}_{ij} = 0$ , the NNN coupling  $\mathcal{J}_2 > 0$  also stabilizes the  $\mathbf{q} = 0$  coplanar structure as mentioned above [46] and thermal Hall effect is present as shown in Fig. 5(b). The easy-plane anisotropy in the XXZ kagomé antiferromagnet also stabilizes the  $\mathbf{q} = 0$  LRO without the DMI. In any case topological spin waves and edge modes are present (see Ref. [45]). Therefore the determination of DMI is immaterial as it does not lead to a finite  $\kappa_{xy}$  in frustrated magnets.

*Conclusion*—. We have shown that geometrical spin frustration on the kagomé antiferromagnets can lead to field-induced scalar spin chirality even in the absence of DMI. The field-induced scalar chirality provides topological spin excitations and thermal Hall response applicable to different frustrated kagomé magnets. These features should be important in many experimentally accessible kagomé antiferromagnets. In particular, frustrated

kagomé jarosites such as  $\text{KCr}_3(\text{OH})_6(\text{SO}_4)_2$  [34, 35] and  $\text{KFe}_3(\text{OH})_6(\text{SO}_4)_2$  [32] meet all the requirements predicted in this report. The presence of scalar spin chirality suggests that there is a high probability that thermal Hall effect will be present in frustrated kagomé QSL materials such as herbertsmithite  $\text{ZnCu}_3(\text{OH})_6\text{Cl}_2$ . This compound has a sizeable DMI ( $\mathcal{D}_z/\mathcal{J} = 0.08$ ) [36] and the ground state is considered as a QSL with spinon continuum excitations [49]. However, the QSL phase in herbertsmithite is fragile in the presence of a magnetic field of about 2 T [38] and a pressure of 2.5 GPa [39]. The chromium compound  $\text{Ca}_{10}\text{Cr}_7\text{O}_{28}$  has also been shown as a QSL candidate [37], but also develops a magnetic order in the presence of a magnetic field [37]. In the disordered QSL regime scalar spin chirality can be spontaneously developed without an applied magnetic field [41–44], whereas in the ordered or frozen regime a magnetic field or pressure can equally induce scalar spin chirality as shown in this paper. Therefore, a finite thermal Hall effect in these magnets should be attributed to scalar spin chirality as opposed to the DMI. A similar effect in frustrated electronic (metallic) magnets is known as topological Hall effect [51–55]. The present model is an analog of

this effect in quantum magnets with charge-neutral magnetic spin excitations. The main result of this report is that a combination of geometrical spin frustration and kagomé antiferromagnets can realize thermal Hall effect without the need of DMI or SOC. Besides, it will be interesting to probe the analogs of “Dirac semimetal” in quantum magnets as pointed out here. The chiral edge modes have not been measured at the moment and they require edge sensitive methods such as light [56] or electronic [57] scattering method. We recently became aware of a recent experimental report of thermal Hall response in frustrated distorted kagomé volborthite at a  $\mathcal{B}$ -field of 15 T with no signs of DMI [58]. However, the exact Hamiltonian for volborthite and its parameter values remain controversial. The results presented here apply specifically to undistorted kagomé antiferromagnets. In this regard, the present study will be important in upcoming experimental studies of finite thermal Hall response in frustrated kagomé magnets.

*Acknowledgements*—. Research at Perimeter Institute is supported by the Government of Canada through Industry Canada and by the Province of Ontario through the Ministry of Research and Innovation.

---

[1] Katsura, H., Nagaosa, N., and Lee, P. A. Theory of the Thermal Hall Effect in Quantum Magnets. *Phys. Rev. Lett.* **104**, 066403 (2010).

[2] Onose, Y. *et al.* Observation of the Magnon Hall Effect. *Science* **329**, 297 (2010).

[3] Matsumoto, R. and Murakami, S. Theoretical Prediction of a Rotating Magnon Wave Packet in Ferromagnets. *Phys. Rev. Lett.* **106**, 197202 (2011). Rotational motion of magnons and the thermal Hall effect. *Phys. Rev. B* **84**, 184406 (2011).

[4] Ideue T. *et al.* Effect of lattice geometry on magnon Hall effect in ferromagnetic insulators. *Phys. Rev. B* **85**, 134411 (2012).

[5] Zhang, L. *et al.* Topological magnon insulator in insulating ferromagnet. *Phys. Rev. B* **87**, 144101 (2013).

[6] Mook, A., Henk, J., and Mertig, I. Edge states in topological magnon insulators. *Phys. Rev. B* **90**, 024412 (2014). Magnon Hall effect and topology in kagome lattices: A theoretical investigation. *Phys. Rev. B* **89**, 134409 (2014).

[7] Matsumoto, R., Shindou, R., and Murakami, S. Thermal Hall effect of magnons in magnets with dipolar interaction. *Phys. Rev. B* **89**, 054420 (2014).

[8] Hirschberger, M. *et al.* Thermal Hall Effect of Spin Excitations in a Kagome Magnet. *Phys. Rev. Lett.* **115**, 106603 (2015).

[9] Chisnell, R. *et al.* Topological Magnon Bands in a Kagome Lattice Ferromagnet. *Phys. Rev. Lett.* **115**, 147201 (2015).

[10] Lee H., Han J. H., and Lee, P.A. Thermal Hall effect of spins in a paramagnet. *Phys. Rev. B* **91**, 125413 (2015).

[11] Boldrin, D. *et al.* Haydeeite: A spin- $\frac{1}{2}$  kagomé ferromagnet. *Phys. Rev. B* **91**, 220408(R) (2015).

[12] Owerre, S. A. A first theoretical realization of honeycomb topological magnon insulator. *J. Phys.: Condens. Matter* **28**, 386001 (2016).

[13] Owerre, S. A. Topological honeycomb magnon Hall effect: A calculation of thermal Hall conductivity of magnetic spin excitations. *J. Appl. Phys.* **120**, 043903 (2016).

[14] Li, F.-Y. *et al.* Weyl magnons in breathing pyrochlore antiferromagnets. *Nat. Commun.* **7**, 12691 (2016).

[15] Mook, A., Henk, J. and Mertig, I. Tunable Magnon Weyl Points in Ferromagnetic Pyrochlores. *Phys. Rev. Lett.* **117**, 157204 (2016).

[16] Ying Su, Wang, X. S., Wang, X. R. Magnonic Weyl semimetal in pyrochlore ferromagnets. *arXiv:1609.01500* (2016).

[17] Owerre, S. A. Field-induced topological magnon and Hall response in honeycomb antiferromagnets. *arXiv:1608.00545* (2016).

[18] Kane, C., and Lubensky, T. C. Topological boundary modes in isostatic lattices. *Nat. Phys.* **10**, 39 (2014).

[19] Chen, B. G., Upadhyaya N., and Vitelli, V. Nonlinear conduction via solitons in a topological mechanical insulator. *Proc. Natl. Acad. Sci. U.S.A.* **111**, 13004 (2014).

[20] Paulose J., Chen B. G., and Vitelli, V. Topological modes bound to dislocations in mechanical metamaterials. *Nat. Phys.* **11**, 153 (2015).

[21] Paulose, J., Meeussen, A. S., and Vitelli, V. Selective buckling via states of self-stress in topological metamaterials. *Proc. Natl. Acad. Sci. U.S.A.* **112**, 7639 (2015).

[22] Rocklin, D. Zeb *et al.* Mechanical Weyl Modes in Topological Maxwell Lattices. *Phys. Rev. Lett.* **116**, 135503 (2016).

[23] Stenull Olaf, Kane, C. L. and Lubensky, T. C. Topological Phonons and Weyl Lines in Three Dimensions. *Phys. Rev. Lett.* **117**, 068001 (2016).

[24] Dzyaloshinsky, I. A thermodynamic theory of “weak” ferromagnetism of antiferromagnetics. *J. Phys. Chem.*

Solids **4**, 241 (1958).

[25] Moriya, T. Anisotropic Superexchange Interaction and Weak Ferromagnetism. Phys. Rev. **120**, 91 (1960).

[26] Chumak, A. V., Vasyuchka, V. I., Serga, Hillebrands, A. A. Magnon spintronics. Nature Phys. **11**, 453 (2015).

[27] Balents, L. Spin liquids in frustrated magnets. Nature **464**, 199 (2010).

[28] Norman, M. R. Colloquium: Herbertsmithite and the search for the quantum spin liquid. Rev. Mod. Phys. **88**, 041002 (2016).

[29] Ran, Y. *et al.* Projected-Wave-Function Study of the Spin-1/2 Heisenberg Model on the Kagomé Lattice. Phys. Rev. Lett. **98**, 117205 (2007).

[30] Elhajal, M., Canals, B., and Lacroix, C. Symmetry breaking due to Dzyaloshinsky-Moriya interactions in the kagomé lattice. Phys. Rev. B **66**, 014422 (2002).

[31] Cépas, O. *et al.* Quantum phase transition induced by Dzyaloshinskii-Moriya interactions in the kagomé antiferromagnet. Phys. Rev. B **78**, 140405(R) (2008).

[32] Grohol, D. *et al.* Spin chirality on a two-dimensional frustrated lattice. Nature Materials **4**, 323 (2005).

[33] Matan, K. *et al.* Spin Waves in the Frustrated Kagomé Lattice Antiferromagnet KFe<sub>3</sub>(OH)<sub>6</sub>(SO<sub>4</sub>)<sub>2</sub>. Phys. Rev. Lett. **96**, 247201 (2006).

[34] Lee, S.-H. *et al.* Less than 50% sublattice polarization in an insulating  $\frac{3}{2}$  kagomé antiferromagnet at  $T \approx 0$ . Phys. Rev. B **56**, 8091 (1997).

[35] Inami, T. *et al.* Magnetic ordering in the kagomé lattice antiferromagnet KCr<sub>3</sub>(OD)<sub>6</sub>(SO<sub>4</sub>)<sub>2</sub>. Phys. Rev. B **64**, 054421 (2001).

[36] Zorko, A. *et al.* Dzyaloshinsky-Moriya Anisotropy in the Spin-1/2 Kagomé Compound ZnCu<sub>3</sub>(OH)<sub>6</sub>Cl<sub>2</sub>. Phys. Rev. Lett. **101**, 026405 (2008).

[37] Balz, C. *et al.* Physical realization of a quantum spin liquid based on a complex frustration mechanism. Nature Phys. **12**, 942 (2016).

[38] Jeong, M. *et al.* Field-Induced Freezing of a Quantum Spin Liquid on the Kagomé Lattice. Phys. Rev. Lett. **107**, 237201 (2011).

[39] Kozlenko, D. P. *et al.* From Quantum Disorder to Magnetic Order in an  $s = 1/2$  Kagomé Lattice: A Structural and Magnetic Study of Herbertsmithite at High Pressure. Phys. Rev. Lett. **108**, 187207 (2012).

[40] Romhányi, J., Penc, K., and Ganesh R. Hall effect of triplons in a dimerized quantum magnet. Nature Communications **6**, 6805 (2015).

[41] Kalmeyer, V. and Laughlin, R. B. Equivalence of the resonating-valence-bond and fractional quantum Hall states. Phys. Rev. Lett. **59**, 2095 (1987).

[42] Wen, X. G., Wilczek, F. and Zee, A. Chiral spin states and superconductivity. Phys. Rev. B **39**, 11413 (1989).

[43] Baskaran, G. Novel local symmetries and chiral-symmetry-broken phases in  $S = 1/2$  triangular-lattice Heisenberg model. Phys. Rev. Lett. **63**, 2524 (1989).

[44] Bauer, B. *et al.* Chiral spin liquid and emergent anyons in a Kagomé lattice Mott insulator. Nature Communications **5**, 5137 (2014).

[45] Supplemental material (<https://arxiv.org/abs/1609.03563>).

[46] Harris, A. B., Kallin, C., and Berlinsky, A. J. Possible Néel orderings of the Kagomé antiferromagnet. Phys. Rev. B **45**, 2899 (1992).

[47] Owerre, S. A., Burkov, A. A., and Melko, R. G. Linear spin-wave study of a quantum kagomé ice. Phys. Rev. B **93**, 144402 (2016).

[48] Steve, M. Y., and Charles L. K. Dirac Semimetals in Two Dimensions. Phys. Rev. Lett. **115**, 126803 (2015).

[49] Han, T. -H. *et al.* Fractionalized excitations in the spin-liquid state of a kagomé-lattice antiferromagnet. Nature **492**, 406 (2012).

[50] Gong, S.-S. *et al.* Global phase diagram of competing ordered and quantum spin-liquid phases on the kagomé lattice. Phys. Rev. B **91**, 075112 (2015).

[51] Taguchi, Y. *et al.* Spin chirality, Berry phase, and anomalous Hall effect in a frustrated ferromagnet. Science **291**, 2573 (2001).

[52] Machida, Y. *et al.* Unconventional Anomalous Hall Effect Enhanced by a Noncoplanar Spin Texture in the Frustrated Kondo Lattice Pr<sub>2</sub>Ir<sub>2</sub>O<sub>7</sub>. Phys. Rev. Lett. **98**, 057203 (2007).

[53] Machida, Y. *et al.* Time-reversal symmetry breaking and spontaneous Hall effect without magnetic dipole order. Nature, **463**, 210 (2008).

[54] Sürgers, C. *et al.* Large topological Hall effect in the non-collinear phase of an antiferromagnet. Nature Commun. **5**, 3400 (2014).

[55] Zhou, J. *et al.* Predicted Quantum Topological Hall Effect and Noncoplanar Antiferromagnetism in K<sub>0.5</sub>RhO<sub>2</sub>. Phys. Rev. Lett. **116**, 256601 (2016).

[56] Ament, Luuk J. P. *et al.* Resonant inelastic x-ray scattering studies of elementary excitations. Rev. Mod. Phys. **83**, 705 (2011).

[57] Zakeri, K. Elementary spin excitations in ultrathin itinerant magnets. Physics Reports **545**, 47 (2014).

[58] Watanabe, D. *et al.* Emergence of nontrivial magnetic excitations in a spin-liquid state of kagomé volborthite. Proc. Natl. Acad. Sci. USA **113**, 8653 (2016).

[59] Holstein, T., and Primakoff, H. Field Dependence of the Intrinsic Domain Magnetization of a Ferromagnet. Phys. Rev. **58**, 1098 (1940).